Inter-Cell Interference Mitigation Allocation for Half-Duplex Relays Based Cooperation

Cédric Abgrall[†‡], Emilio Calvanese Strinati[†] and Jean-Claude Belfiore[‡]
Email: cedric.abgrall@cea.fr, emilio.calvanese-strinati@cea.fr and jean-claude.belfiore@telecom-paristech.fr

[†] CEA, LETI, MINATEC
17, rue des Martyrs - 38054 Grenoble, France

[‡]TELECOM ParisTech (ENST)
46, rue Barrault - 75013 Paris, France

Abstract

***Abstract*—Inter-cell interference is one of the most limiting problems in high capacity mobile wireless networks. The goal of our work is to limit inter-cell interference in two-hop cooperative communication systems, by exploiting the half-duplex per chunk property of relays. Such relays cannot be interfered on a chunk while they are transmitting on it. Cooperative communications may improve the reliability of transmissions, but can also be prejudicial if relays are strongly interfered. Furthermore, additional inter-cell interference is introduced by cooperative communications. For these reasons we propose novel resource allocation modes for such relays; our modes try to protect relays from inter-cell interference and reduce energy needs. We compare our proposals to modes based on classical design. Simulation results show how our proposed allocation modes permit to outperform classical modes in terms of cooperation effectiveness, power consumption and perceived Quality of Service.**

I. Introduction

Nowadays, wireless networks target always higher requirements (capacity, coverage, etc.) while available radio resources become more and more scarce and have to be shared. This cause intra- and inter-cell interference that must be mitigated to guarantee the coexistence of simultaneous transmissions.

Several methods have been investigated to cope with the interference issue. First, transmissions can be made orthogonal by convenient allocations of time and frequency resource. See *Frequency Reuse* techniques for instance [1]. Second, signal processing can help in coping with interference. *Interference Avoidance* (*e.g. Dirty Paper Coding*) and *Interference Cancellation* (*SIC*) are possible solutions. A fashionable technique is *Interference Alignment* [2]. Each system disposes of a limited amount of degrees of freedom. Some of them are 'sacrificed' to align interfering signals on them; the other degrees of freedom are eventually interference-free. Third, techniques based on optimization under constraints are also well-suited to our issue [3]. For instance, the well-known *Water-Filling* is an illustration of *Power Control* techniques [4].

In this paper we focus on two-hop cooperative based communications. If they may enhance reliability of communications, they also suffer from some drawbacks: amplified noise with AF protocol, erroneous decoding with DF protocol for instance. Besides, cooperative transmissions introduce additional interfering transmitters in the system and can possibly enhance perceived interference level. We propose here a novel resource allocation strategy for *half-duplex* relays, *i.e.*, relays cannot transmit and listen simultaneously. In case of OFDMA systems, relays can be *half-duplex per chunk*, *i.e.*, a relay is *half-duplex* for a given chunk but its behaviour on each chunk is independent: relays are able to listen on a chunk while they are transmitting on another. Furthermore, intra-cell interference can be easily avoided with orthogonal allocations between users of the same cell in case of OFDMA systems.

The remaining of the paper is organized as follow. In Section II we briefly describe our system model and notations. Classical resource allocation modes and our proposed versions are developed in Section III. Section IV introduces our simulation methodology and Section V shows simulation results. Section VI concludes this paper.

II. System Model and Notations

In this section, notations and system model adopted in the rest of the paper are introduced. The considered system is shown on Figure 1 and accounts of tri-sectorized cells of radius r_{cell}. Our analysis is focused on three adjacent sectors.

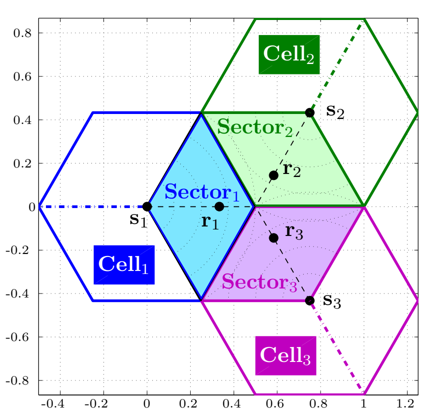

Fig. 1: System model with three adjacent sectors

Each sector, denoted by S_i, consists of a source $\mathbf{s}_i$ (base station for downlink transmissions), a single user equipment $\mathbf{d}_i$ as destination and a single relay station $\mathbf{r}_i$. Relays are fixed and all have the same location relative to their sector: relays are placed at two thirds of r_{cell} from their base station, on the symmetry axis of the sector. All network agents are equipped with only one antenna. Relays work in half-duplex per chunk mode; they further can be active or remain silent for a given transmission.

Each transmission can be done on maximum N_{chunks} frequency chunks. Channel gains and transmit powers are relative to a given chunk and are identified by the chunk's index in exponent between brackets (omitted if referring to all chunks or if equality between chunks). Source $\mathbf{s}_i$ and relay $\mathbf{r}_i$ transmit respectively with powers $P_{s_i}^{(k)}$ and $P_{r_i}^{(k)}$ on chunk k. Channels between $\mathbf{s}_i$ and $\mathbf{d}_j$, $\mathbf{r}_i$ and $\mathbf{d}_j$, $\mathbf{s}_i$ and $\mathbf{r}_j$ are respectively denoted by coefficients $f_{ij}^{(k)}$, $g_{ij}^{(k)}$ and $h_{ij}^{(k)}$, on chunk k. These coefficients represent the global gain of channels, including fading, shadowing and path loss attenuation. They remain constant during at least one frame transmission. Fading follows a Rayleigh distribution with unitary expectation. Log-normal shadowing is generated using the method described in [5]. Path loss model is the one of Okumura-Hata with $\text{PL}_{\text{dB}} = L + k.log_{10}(d)$ in dB, d [km] is the distance between transmitter and receiver. Transmitters are assumed to have perfect knowledge of all channel gains.

A schematic illustration of the two-hop channel model for one sector S_i is given on Figure 2. $\mathbf{d}_i$ and $\mathbf{r}_i$ are respectively subject to both AWGN noise (with variance $\sigma_{d_i}^2$ and $\sigma_{r_i}^2$), and inter-sector interference I_i and J_i. Relays can perform both *Orthogonal Decode and Forward* (ODF) or *Orthogonal Amplify and Forward* (OAF) protocols. These cooperative protocols are said 'Orthogonal' since resources for both hops' transmissions are orthogonally allocated (separation in time and/or frequency). Both OAF and ODF cooperative protocols are commonly adopted for almost all cooperative transmissions based systems.

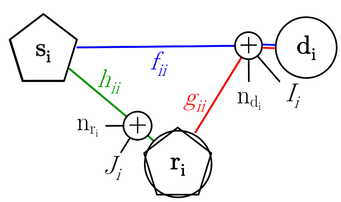

Fig. 2: System model for the set $\{\mathbf{s}_i,\mathbf{r}_i,\mathbf{d}_i\}$

III. Description of Resource Allocation Modes

Three strategies of time and frequency resources allocation are introduced and then investigated: *Classic*$_1$ (C1), *Classic*$_2$ (C2) and *Advanced* (A). *Classic*$_1$ and *Classic*$_2$ strategies assign time and frequency resources to neighbour sectors according to conventional techniques, while our proposed *Advanced* strategy is more spectral efficient and exploits the half-duplex per chunk property of relays. For an easier explication, allocation designs are presented hereafter for only two frequency chunks ($N_{chunks} = 2$). Sectors do not perform Power Control techniques, they do not attempt to optimize their transmit power. On the other hand, a simple 'On-Off' power allocation is applied between sectors to sources and relays. Indeed, sources and relays either do not transmit, or transmit respectively at power $P_{s_i}^{(k)}$ and $P_{r_i}^{(k)}$. This principle is introduced in [6] and is shown to be near optimal. It is however not introduced for cooperative transmissions. More chunks and any Power Control mechanisms can be combined to our examples.

Notation is the following. Each allocation pattern is labelled with 3 letters and an index. First letter refers to sector S_1, second to sector S_2 and third to sector S_3, while the index indicates the allocation strategy ('C1', 'C2' or 'A'). Each letter indicates either if in the *i-th* sector cooperation ('C') or no cooperation ('N') is planned. Thus, 2^3 families of allocation modes are defined for each of the 3 strategies (3 sectors with each two possibilities: 'C' or 'N').

Figures 3, 4 and 5 show the most representative allocation modes (packet index in exponent). Patterns are represented as follows: rows and columns are respectively divided into time slots and frequency chunks that can be either assigned to only one transmitter, or shared. See for instance the mode NNN_{C1} on Figure 3a: the second chunk is shared. If a resource is exclusively assigned to one transmission, then this transmission is interference free. However if a resource is shared, then the simultaneous communications will suffer from inter-site interference.

A. *Classic*$_1$ strategy of allocation modes (C1)

With *Classic*$_1$ strategy, when resource allocation is scheduled, one chunk is granted one sector (S_1 for instance), while the other chunk is shared by the remainder two sectors (S_2 and S_3 for instance). Hence, one sector is advantaged in terms of inter-site interference. Therefore, in our examples, S_1 is interference free, while destinations $\mathbf{d}_2$ and $\mathbf{d}_3$ are interfered by transmissions occurring respectively in sector S_3 and in sector S_2. Channel capacity's expression can be specifically derived for each allocation mode. When no sector plans cooperation (NNN_{C1}), the amount of mutual information $\mathscr{I}_{\text{NNN}_{\text{C1}}}^i$ for sector S_i can be derived as:

$$
\begin{aligned}
\mathscr{I}_{\text{NNN}_{\text{C1}}}^1 &= \log_2\left(1 + \frac{P_{s_1}^{(1)} f_{11}^{(1)}}{\sigma_{d_1}^2}\right) \\
\mathscr{I}_{\text{NNN}_{\text{C1}}}^i &= \log_2\left(1 + \frac{P_{s_i}^{(2)} f_{ii}^{(2)}}{\sigma_{d_i}^2 + P_{s_j}^{(2)} f_{ji}^{(2)}}\right) \\
& i \neq j, \quad (i,j) = \{2,3\}
\end{aligned}
$$

Neighbour transmissions are synchronized: active transmitters (sources, relays) in S_2 and S_3 simultaneously broadcast on the second chunk. If cooperation is planned in S_2 or S_3 (Figures 3c–3f), relay's listening phase is interfered by transmissions of the neighbour source. Relays have better not to cooperate if the signal they listen to is too interfered. The amount of mutual information $\mathscr{I}_{\text{NCN}_{\text{C1}}}^2$ for NCN_{C1} mode is derived below for OAF and ODF protocols (see [7]). Most illustrative *Classic*$_1$ allocation modes are shown on Figure 3.

B. *Classic*$_2$ strategy of allocation modes (C2)

With *Classic*$_2$ allocation modes, there is no frequency planning between sectors: both chunks are assigned to all sectors. Therefore, each destination suffers, on both chunks, from interference caused by neighbour active transmitters ($\mathbf{s}_i$ or $\mathbf{r}_i$). When cooperation is planned in a sector, relay's listening phase is interfered by transmission of neighbour

$$\mathscr{I}^{2,\mathrm{AF}}_{\mathrm{NCN_{C1}}} = \log_2\left(1 + \frac{P^{(2)}_{s_2} f^{(2)}_{22}}{\sigma^2_{d_2} + P^{(2)}_{s_3} f^{(2)}_{32}} + \frac{P^{(2)}_{s_2} h^{(2)}_{22} P^{(2)}_{r_2} g^{(2)}_{22}}{\left(\sigma^2_{d_2} + P^{(2)}_{s_3} f^{(2)}_{32}\right) . \left(\sigma^2_{r_2} + P^{(2)}_{s_2} h^{(2)}_{22} + P^{(2)}_{s_3} f^{(2)}_{32}\right) + P^{(2)}_{r_2} g^{(2)}_{22} . \left(\sigma^2_{r_2} + P^{(2)}_{s_3} f^{(2)}_{32}\right)}\right)$$

$$\mathscr{I}^{2,\mathrm{DF}}_{\mathrm{NCN_{C1}}} = \log_2\left(1 + \frac{P^{(2)}_{s_2} f^{(2)}_{22}}{\sigma^2_{d_2} + P^{(2)}_{s_3} f^{(2)}_{32}} + \frac{P^{(2)}_{r_2} g^{(2)}_{22}}{\sigma^2_{r_2} + P^{(2)}_{s_3} f^{(2)}_{32}}\right)$$

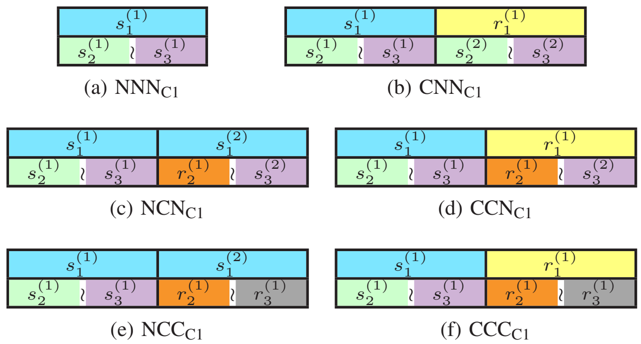

(a) $\mathrm{NNN_{C1}}$ (b) $\mathrm{CNN_{C1}}$ (c) $\mathrm{NCN_{C1}}$ (d) $\mathrm{CCN_{C1}}$ (e) $\mathrm{NCC_{C1}}$ (f) $\mathrm{CCC_{C1}}$

Fig. 3: Patterns of allocation modes for *Classic*$_1$ strategy

sources. In comparison to *Classic*$_1$ allocation modes, relays and destinations encounter more interference, but sources and relays transmit in return on both chunks. Most illustrative modes are shown on Figure 4.

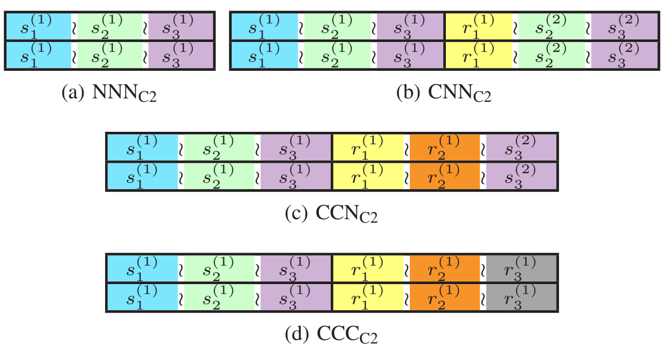

(a) $\mathrm{NNN_{C2}}$ (b) $\mathrm{CNN_{C2}}$ (c) $\mathrm{CCN_{C2}}$ (d) $\mathrm{CCC_{C2}}$

Fig. 4: Patterns of allocation modes for *Classic*$_2$ strategy

Amount of mutual information $\mathscr{I}^i_{\mathrm{NNN_{C2}}}$ for sector S_i and mode $\mathrm{NNN_{C2}}$ is derived as:

$$\begin{aligned} \mathscr{I}^i_{\mathrm{NNN_{C2}}} = & \log_2\left(1 + \frac{P^{(1)}_{s_i} f^{(1)}_{ii}}{\sigma^2_{d_i} + P^{(1)}_{s_j} f^{(1)}_{ji} + P^{(1)}_{s_k} f^{(1)}_{ki}}\right) \\ + & \log_2\left(1 + \frac{P^{(2)}_{s_i} f^{(2)}_{ii}}{\sigma^2_{d_i} + P^{(2)}_{s_j} f^{(2)}_{ji} + P^{(2)}_{s_k} f^{(2)}_{ki}}\right) \\ i \neq j \neq k, & \quad (i,j,k) = \{1,2,3\} \end{aligned}$$

C. Proposed Advanced strategy of allocation modes (A)

This strategy is designed for half-duplex per chunk relays. Source $\mathbf{s}_i$ transmits on a chunk the packet m_k, relay $\mathbf{r}_i$ listens to m_k on this chunk while transmits the packet m_{k-1} on the other chunk. Transmission of one single packet always requires two time slots, but for n packets it needs $(n+1)$ time slots, which asymptotically tends to n.

The allocation patterns which are investigated hereafter are thus reduced to one time slot (two time slots with classical strategies). When resource allocation is scheduled, one chunk is granted one source ($\mathbf{s}_1$ for instance), while remainder sources ($\mathbf{s}_2$ and $\mathbf{s}_3$ for instance) share the other chunk. Hence, one source is advantaged in term of inter-sector interference. Assume below that $\mathbf{s}_1$ is the advantaged source. Destination $\mathbf{d}_1$ is interfered on the first chunk by neighbour relays, only if S_2 or S_3 plans cooperation. Destinations $\mathbf{d}_2$ and $\mathbf{d}_3$ are interfered on the second chunk respectively by $\mathbf{s}_3$ and $\mathbf{s}_2$, but also by $\mathbf{r}_1$ if S_1 plans cooperation.

When no sector plans cooperation, $\mathrm{NNN_A}$ mode is defined as $\mathrm{NNN_{C1}}$ (Figure 3a). If S_1 plans cooperation, $\mathbf{r}_1$'s listening phase on the first chunk is interfered by neighbour relays' transmissions, only if S_2 or S_3 plans cooperation too (see Figures 5a, 5c and 5e); on the other hand, $\mathbf{d}_1$ is always interfered by $\mathbf{s}_2$ and $\mathbf{s}_3$ on the second chunk. The amount of mutual information $\mathscr{I}^1_{\mathrm{CNN_A}}$ in sector S_1 for $\mathrm{CNN_A}$ mode is derived for respectively OAF and ODF protocols as:

$$\begin{aligned} \mathscr{I}^{1,\mathrm{AF}}_{\mathrm{CNN_A}} = & \log_2\left(1 + \frac{P^{(1)}_{s_1} f^{(1)}_{11}}{\sigma^2_{d_1}}\right) \\ + & \log_2\left(1 + \frac{P^{(1)}_{s_1} h^{(1)}_{11} . P^{(2)}_{r_1} g^{(2)}_{11}}{P^{(2)}_{r_1} g^{(2)}_{11} + \left(\sigma^2_{d_1} + P^{(1)}_{s_1} h^{(1)}_{11}\right) . X}\right) \\ \text{with } X = & \sigma^2_{r_1} + P^{(2)}_{s_2} f^{(2)}_{21} + P^{(2)}_{s_3} f^{(2)}_{31} \\ \mathscr{I}^{1,\mathrm{DF}}_{\mathrm{CNN_A}} = & \log_2\left(1 + \frac{P^{(1)}_{s_1} f^{(1)}_{11}}{\sigma^2_{d_1}}\right) \\ + & \log_2\left(1 + \frac{P^{(2)}_{r_1} g^{(2)}_{11}}{\sigma^2_{r_1} + P^{(2)}_{s_2} f^{(2)}_{21} + P^{(2)}_{s_3} f^{(2)}_{31}}\right) \end{aligned} \quad (1)$$

If S_2 plans cooperation (likewise for S_3, by symmetry), relay $\mathbf{r}_2$'s listening phase on the second chunk is interfered by $\mathbf{s}_3$, but also by $\mathbf{r}_1$ if S_1 plans cooperation too. $\mathbf{d}_2$ is always interfered on the first chunk by $\mathbf{s}_1$, but also by $\mathbf{r}_3$ if S_3 plans cooperation. Most illustrative modes are shown on Figure 5.

IV. Simulation Process and Assumptions

In this section we describe the adopted process for our simulations and the assumptions we made. Relay based transmissions in cooperative networks may improve channel capacity, but also enhance inter-sector interference and possibly overall transmit power. Furthermore, an optimal allocation mode for a given communication context (fading, shadowing, path loss attenuation) can be suboptimal with another context, since perceived inter-sector interference level is specific to

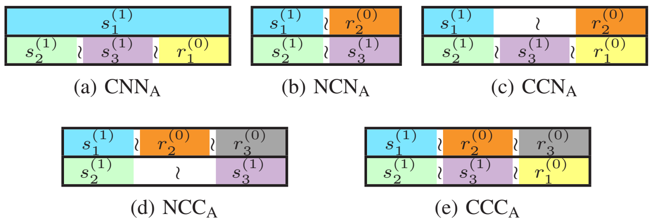

Fig. 5: Patterns of allocation modes for *Advanced* strategy

each allocation mode. Therefore performance of all modes introduced in Section III are evaluated under several channel realizations (fading and shadowing) and for different locations of destinations (leading to different path loss attenuations). The adopted metric for our study is based on the sum of mutual information amount of each sector (*GMI: Global Mutual Information*). So as to take account of time, frequency and space variations of transmission scenarios, *GMI* is averaged on distinct random communication contexts. $\overline{GMI}$ stands for the averaged overall amount of mutual information.

In this paper, results are shown from the viewpoint of sector S_1. Hereafter an application context is given for such results. Assume that sector S_1 tries to assign its transmission resources so as to maximize *GMI* of the system, and not necessarily its own amount of mutual information $\mathscr{I}^1$. Assume also that S_1 has neither knowledge of the location of $\mathbf{d}_2$ and $\mathbf{d}_3$, nor knowledge of channel states. Consequently, S_1 should assign its transmission resources according to an averaged communication context. The only parameter to which S_1 has access is the location of its destination $\mathbf{d}_1$. Therefore results will be introduced according to the location of $\mathbf{d}_1$.

A $n_{\text{step}} \times n_{\text{step}}$ grid parcels out each sector. Hereafter the 4 steps of our simulation process are developed, for a given location of $\mathbf{d}_1$ on its grid:

- N_{pos} positions for $\mathbf{d}_2$ in S_2 and N_{pos} positions for $\mathbf{d}_3$ in S_3 are randomly chosen.
- N_{chan} channel states including fading and shadowing are randomly computed for all links.
- For each of these $N_{pos}.N_{chan}$ distinct communication contexts, $GMI_{\mathbf{d}_1}$ is computed for each allocation mode.
- Our metric $\overline{GMI}_{\mathbf{d}_1}$ is computed by averaging $GMI_{\mathbf{d}_1}$ on these $N_{pos}.N_{chan}$ distinct communication contexts.

Allocation modes of the 3 strategies (C1, C2 and A) are evaluated for both OAF and ODF cooperative protocols. With OAF protocol, the amplification gain is defined such that transmission power equals P_{r_i}; while with ODF protocol, relays are assumed to decode their signal without error. System model and algorithm settings adopted in our numerical results are summarized in Table I.

System model		Algorithm
$P_{s_i} = 10W$	$N_{chunks} = 2$	$N_{pos} = 1000$
$P_{r_i} = 1W$	$\sigma^2_{d_i} = \sigma^2_{r_i} = -105\text{dBm}$	$N_{chan} = 500$
$r_{\text{cell}} = 0.5\text{km}$	$\text{PL}_{\text{dB}} = 137.74 + 30.\log_{10}(d), d[\text{km}]$	$n_{\text{step}} = 20$

TABLE I: System Model and Algorithm Settings

V. Simulation Results

Simulation results are shown for both classical and proposed allocation modes. Performance are compared with 2 different metrics: first the introduced metric $\overline{GMI}_{\mathbf{d}_1}$, second in terms of both $\overline{GMI}_{\mathbf{d}_1}$ and power consumption. This second metric will be referred to by $\widehat{GMI}_{\mathbf{d}_1}$. If the first criterion of comparison is in accordance with the common goal in Information Theory, *i.e.,* maximization of channel capacity, the second criterion is more compliant with constraints of present wireless networks.

Figures show the evolution of $\overline{GMI}_{\mathbf{d}_1}$ or $\widehat{GMI}_{\mathbf{d}_1}$ with the increasing distance between $\mathbf{s}_1$ and $\mathbf{d}_1$: mobility of destination $\mathbf{d}_1$ is constrained to the axis ($\mathbf{s}_1$–$\mathbf{r}_1$). Dotted, dashed and solid curves represent respectively results for *Classic*$_1$, *Classic*$_2$ and *Advanced* allocation modes. Each family of modes is identified by a specific marker and a specific color: NNN (red curve, no marker), CNN (green curve, upward-pointing triangle), NCN (blue curve, downward-pointing triangle), CCN (magenta curve, circle), NCC (gray curve, plus sign) and CCC (black curve, five-pointed star). Results for families NNC and CNC are identical respectively to those of families NCN and CCN (by design symmetry) and are thus not shown.

A. *Evolution of $\overline{GMI}_{\mathbf{d}_1}$: Without Energy Constraints*

In this subsection we compare classical modes to advanced modes with our before introduced metric $\overline{GMI}_{\mathbf{d}_1}$. Results describe an ideal case where transmissions are not constrained by system limitations. For each allocation mode, we investigate which overall amount of mutual information can be reached. On Figures 6 (OAF) and 7 (ODF) we plot the evolution of $\overline{GMI}_{\mathbf{d}_1}$ along the axis ($\mathbf{s}_1$–$\mathbf{r}_1$). Results for *Classic*$_1$ modes are not shown, since they are always outperformed by *Classic*$_2$ modes.

Mobility of $\mathbf{d}_1$ does not impact mutual information amount of sectors S_2 and S_3. As expected due to path loss attenuation, the farer is $\mathbf{d}_1$ from $\mathbf{s}_1$, the lower is the amount of mutual information for S_1, and thus $\overline{GMI}_{\mathbf{d}_1}$. However, when S_1 plans cooperation (CNN, CCN, CCC families), $\overline{GMI}_{\mathbf{d}_1}$ improves close to $\mathbf{r}_1$ (dist($\mathbf{s}_1$,$\mathbf{d}_1$)=0.33km). With our assumptions, ODF protocol cancels interference while OAF protocol amplifies interference. $\overline{GMI}_{\mathbf{d}_1}$ enhancements in the vicinity of $\mathbf{r}_1$ are therefore bigger with ODF protocol (Fig. 7) than with OAF (Fig. 6). We observe that *Classic*$_2$ modes outperform *Advanced* modes when $\mathbf{d}_1$ is out of reach of $\mathbf{r}_1$. However benefits of cooperative transmissions are greater in the surroundings of $\mathbf{r}_1$ with *Advanced* modes than with *Classic*$_2$. Furthermore, in case of OAF protocol, $\mathrm{CNN_A}$ mode is the only cooperative mode of interest around $\mathbf{r}_1$.

Eventually, results of our proposed *Advanced* modes with half-duplex per chunk relays are sometimes far below those of *Classic*$_2$ modes (especially when $\mathbf{d}_1$ is near to $\mathbf{s}_1$). But the real novelty brought by the *Advanced* strategy is not pointed up with the metric $\overline{GMI}_{\mathbf{d}_1}$. Indeed modes are not constrained in power: there is here no drawback to allocate too many resources to transmitters.

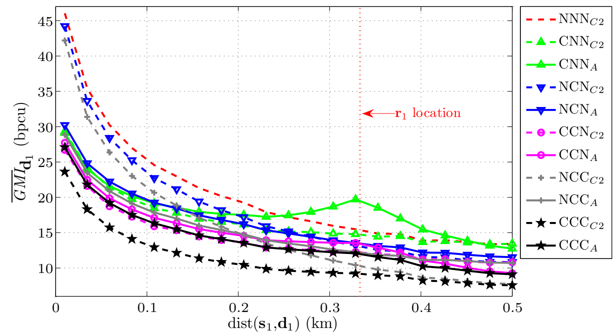

Fig. 6: $\overline{GMI}_{\mathbf{d}_1}$ variations along ($\mathbf{s}_1$–$\mathbf{r}_1$) axis, OAF protocol

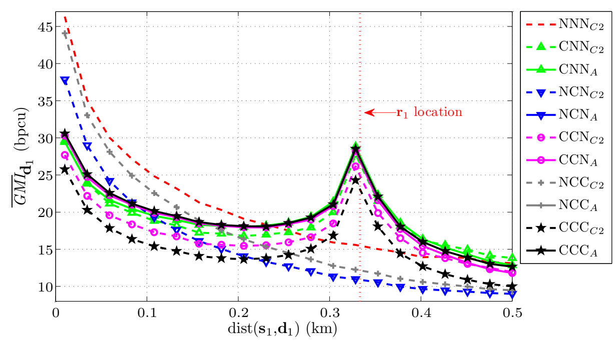

Fig. 7: $\overline{GMI}_{\mathbf{d}_1}$ variations along ($\mathbf{s}_1$–$\mathbf{r}_1$) axis, ODF protocol

B. Evolution of $\widehat{GMI}_{\mathbf{d}_1}$: With Energy Constraints

The race against the maximization of mutual information has a price that must be taken into account. In wireless systems, transmissions are power limited by material constraints but also for assuring the coexistence of various systems that are sharing the same resources. A major consideration is brought to power consumption because in some cases it is the critical bottleneck: transmitters cannot behave selfishly and transmit at full power, power has to be carefully set [8].

In this subsection we investigate the energy needs of all investigated allocation modes. New transmitters (relays) are added with cooperative modes: even if cooperative transmissions could enhance the overall amount of mutual information, this enhancement should not be done at the expense of huge energy needs. The idea here is to consider jointly the overall amount of mutual information (GMI) and the energy needs of each allocation mode. Based on transmission pattern of modes, the power price of all modes is easily computed. For instance, Table II gives these energy needs in case of equal transmission power constraints for 3 sources and 3 relays. Power price depends on the number, the nature and the power of the transmitters, as well as the number of frequency bands used by each of them. As we can see, our protocols considerably save power.

	NNN	CNN,NCN,NNC	CCN,CNC,NCC	CCC
C1	$3.P_s$	$5.P_s$+P_r	$2(2.P_s$+$P_r)$	$3(P_s$+$P_r)$
C2	$6.P_s$	$2(5.P_s$+$P_r)$	$4(2.P_s$+$P_r)$	$6(P_s$+$P_r)$
A	$3.P_s$	$3.P_s$+P_r	$3.P_s$+$2.P_r$	$3(P_s$+$P_r)$

TABLE II: Overall transmit power per allocation mode, with equal powers P_s and P_r between sectors and chunks.

A new metric is introduced, $\widehat{GMI}_{\mathbf{d}_1}$, which stands for the weighting of ($\overline{GMI}_{\mathbf{d}_1}$) by the energy needs of the considered allocation mode. On Figures 8 (OAF) and 9 (ODF) we plot the evolution of $\widehat{GMI}_{\mathbf{d}_1}$ along the axis ($\mathbf{s}_1$–$\mathbf{r}_1$). Results for *Classic*$_2$ modes are not shown, since both *Classic*$_1$ and *Advanced* modes outperform *Classic*$_2$ ones. As previous results, $\widehat{GMI}_{\mathbf{d}_1}$ decreases with the increasing distance between $\mathbf{s}_1$ and $\mathbf{d}_1$, except in the vicinity of $\mathbf{r}_1$ where CNN, CCN and CCC families of modes enhance $\widehat{GMI}_{\mathbf{d}_1}$. As before, ODF protocol leads to greater enhancements than OAF protocol around $\mathbf{r}_1$. When $\mathbf{d}_1$ is out of reach of $\mathbf{r}_1$ (dist($\mathbf{r}_1$,$\mathbf{d}_1$)$\gtrsim$0.11km), NNN$_{C1}$ allocation mode (also used as NNN$_A$) outperforms other modes, for both OAF and ODF protocols. The novelty with Figures 8 and 9 is that our *Advanced* allocation modes substantially outperform classical strategies. We further observe that the smaller is the number of sectors in which cooperation is activated, the higher is the $\widehat{GMI}_{\mathbf{d}_1}$.

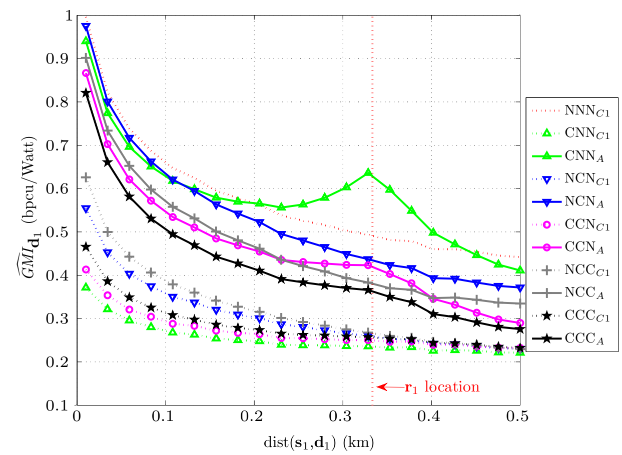

Fig. 8: $\widehat{GMI}_{\mathbf{d}_1}$ variations along ($\mathbf{s}_1$–$\mathbf{r}_1$) axis, OAF protocol

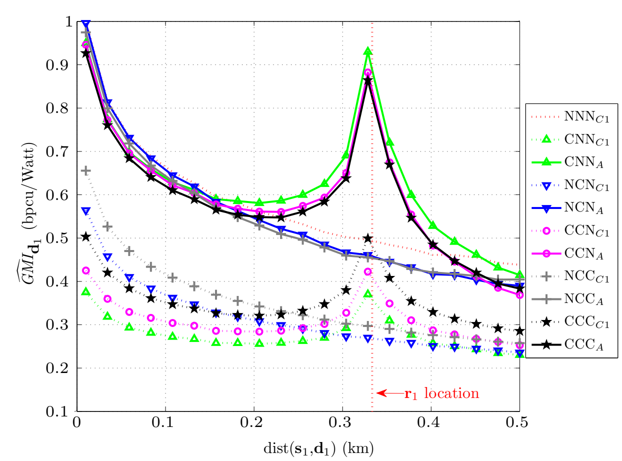

Fig. 9: $\widehat{GMI}_{\mathbf{d}_1}$ variations along ($\mathbf{s}_1$–$\mathbf{r}_1$) axis, ODF protocol

Previous results show $\widehat{GMI}_{\mathbf{d}_1}$ variations when $\mathbf{d}_1$ was constrained to move along ($\mathbf{s}_1$–$\mathbf{r}_1$) axis. Figures 10–12 show how $\widehat{GMI}_{\mathbf{d}_1}$ variates when $\mathbf{d}_1$ occupies all positions on the $n_{\text{step}} \times n_{\text{step}}$ grid that parcels out sector S_1. For lack of space, we limit us to ODF protocol and to the 2 best allocation modes on Figure 9: NNN$_{C1}$ mode (*i.e.,* NNN$_A$) (Fig. 10) and

$\mathrm{CNN_A}$ mode (Fig. 11). As a rough guide, we also plot results for $\mathrm{CNN_{C1}}$ mode (Fig. 12). On Figure 10 $\widehat{GMI}_{\mathbf{d}_1}$ decreases isotropically with increasing distance between $\mathbf{s}_1$ and $\mathbf{d}_1$ (the inverse of the cubed distance, see Table I). On the other hand, decrease of $\widehat{GMI}_{\mathbf{d}_1}$ is not isotropically any more on Figure 11: as soon as $\mathbf{d}_1$ is out of reach of either $\mathbf{s}_1$ or $\mathbf{r}_1$, $\widehat{GMI}_{\mathbf{d}_1}$ rapidly falls off. We further observe that cell-edge users do not particularly profit from cooperative transmissions. But in comparison to classical modes (see Fig. 12 and more particularly the graduations of the colour bar on the right), areas where cooperation ameliorates performance are enlarged. Results obtained with OAF protocol are quite similar, $\widehat{GMI}_{\mathbf{d}_1}$ is just less increased in the vicinity of $\mathbf{r}_1$.

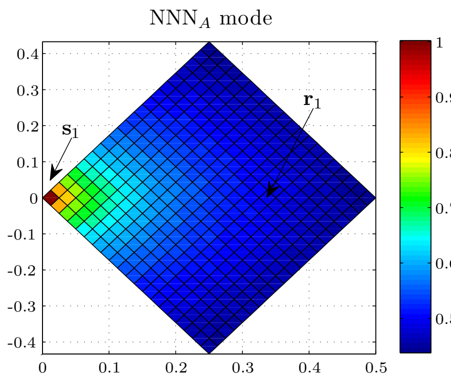

Fig. 10: $\widehat{GMI}_{\mathbf{d}_1}$ variations on sector S_1 for $\mathrm{NNN_A}$ mode (ODF)

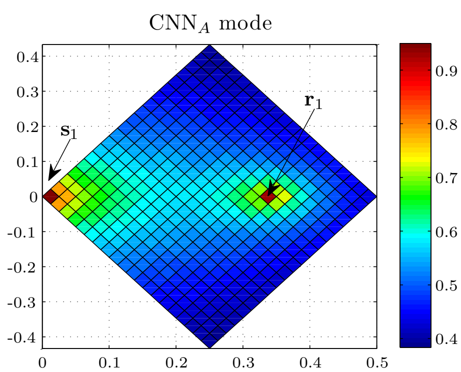

Fig. 11: $\widehat{GMI}_{\mathbf{d}_1}$ variations on sector S_1 for $\mathrm{CNN_A}$ mode (ODF)

Eventually, we understand better the advantages of our modes that combine both lower power consumption and efficiency of inter-site resource allocation. *Classical*$_2$ strategy does not perform inter-sector interference aware resource allocation and furthermore requires huge energy needs: it is consequently the worst strategy with this second metric. Finer comparisons between modes prove that *Advanced* modes outperform everywhere in sector S_1 classical modes.

VI. Conclusion

These paper proposes novel efficient inter-sector resource allocation modes for two-hop cooperative communication systems, where relays are half-duplex per chunk. Numerical evaluations compare the proposed solutions to allocation modes with classical management of resource that do not integrate inter-sector interference techniques in their design. Simulations results show that advantages of *Advanced* modes are twofold. First, overall energy needs is substantially lowered in comparison to *Classic*$_2$ modes. Second, by protecting relays from inter-sector interference, cooperative transmissions permit to increase the global amount of mutual information in all investigated communication scenarios. We further observe that the proposed solutions lead to an extension of the areas where cooperation profits to destinations. Cell-edge users are always out of reach of transmitters, but their perceived Quality of Service is increased: inter-sector interference is consequently lowered. Further work will focus on an adaptive resource allocation which would be aware of inter-sector interference issue.

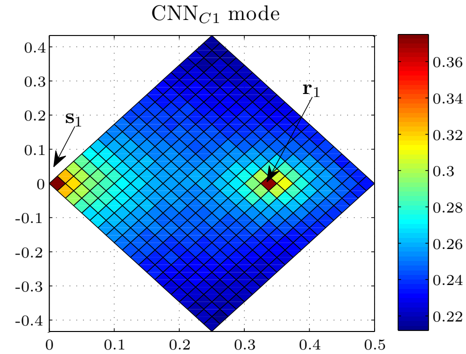

Fig. 12: $\widehat{GMI}_{\mathbf{d}_1}$ variations on sector S_1 for $\mathrm{NNN_{C1}}$ mode (ODF)

Acknowledgments

This work has been performed in the framework of the FP7 project ROCKET IST-215282 STP, which is funded by the European Community.

References

[1] Y. Xiang, J. Luo and C. Hartmann, “Inter-Cell Interference Mitigation through Flexible Resource Reuse in OFDMA based Communication Networks,” *Proc. European Wireless 2007*, pp. 1–7, Apr. 2007.

[2] K. Gomadam, V.R. Cadambe and S.A. Jafar, “Approaching the capacity of wireless networks through distributed interference alignment,” *IEEE GLOBECOM 2008*, pp. 1–6, Nov. 2008.

[3] S. Boyd and L. Vandenberghe, “Convex optimization,” Cambridge University Press, Mar. 2004.

[4] T.M. Cover and J.A. Thomas, “Elements of Information Theory,” Wiley-Interscience, 2nd Edition, Jul. 2006.

[5] X. Cai and G. Giannakis, “A two-dimensional channel simulation model for shadowing processes,” *IEEE Trans. Vehicular Technology*, vol. 52, no. 6, pp. 1558–1567, Nov. 2003.

[6] D. Gesbert, S.G. Kiani, A. Gjendemsjo and G.E. Oein, “Adaptation, coordination and distributed resource allocation in interference-limited wireless networks,” *IEEE Proc.*, vol. 95, no. 12, pp. 2393–2409, Dec. 2007.

[7] Z. Yong, L. Jun, X. Youyun and C. Yueming, “An adaptive non-orthogonal cooperation scheme based on channel quality information,” *IEEE WiCom 2007*, pp. 988–991, Sep. 2007.

[8] [EARTH] FP7-ICT-2009-4 Project EARTH, Grant Agreement 247733.